Robust PCA for Through-the-Wall Radar Imaging

Hugo Brehier[1], Arnaud Breloy[2], Chengfang Ren[1], Israel Hinostroza[1], and Guillaume Ginolhac[3]

[1]SONDRA, CentraleSupélec, Paris-Saclay University, France
[2]LEME, Paris Nanterre University, France
[3]LISTIC, Savoie Mont-Blanc University, France

***Abstract*—Through-the-wall radar imaging (TWRI) is an ongoing field of research which aims at investigating the inside of a building from its outside. In the most common setting, it seeks to detect or monitor stationary targets. Departing from usual delay-and-sum techniques, sparse recovery problems have been proposed to solve this detection problem. These methods rely on a preprocessing step where an appropriate separation of wall and target subspaces is first performed to remove the front wall response. In this work, we explore one-step methods using joint low-rank and sparse decomposition methods through the Robust PCA (RPCA) framework. The novelty is a one-step recovery from a structured inversion problem for which we tailor an Alternating Direction Method of Multipliers (ADMM) algorithm. We validate and compare our method on simulations.**

***Index Terms*—Through-the-wall radar, RPCA, detection, inversion**

I. Introduction

Through-the-wall radar imaging (TWRI) [1] aims at investigating the inside of a building using electromagnetic (EM) waves emitted from its outside, making use of their penetrating properties to pass through walls. Most commonly, a single room is considered, consisting of a front wall behind which the radar is placed, and inner walls delimiting the imaged scene from which we seek to detect and classify targets. TWRI is useful in both military operations and civilian applications, such as emergency relief. It is a challenging task as the backscattered signal from targets is strongly attenuated by the front wall. Moreover, it contains strong interferences from the front wall as well as clutter from inner walls. The signal is also distorted by multipath which complicates the task of target detection.

Traditional techniques to create detection maps in radar comprise Generalized Likelihood Ratio Tests (GLRTs) [2], to test the hypothesis of a target being present at a given position, as well as delay-and-sum beamforming approaches, such as the Synthetic Aperture Radar (SAR) algorithm of Back Projection (BP) [3]. However, this does not allow for the physical characteristics of the imaged scene to be taken into account (through wall effects, multipath).

More recent works have proposed a structured recovery/regression problem through a dictionary mapping the signal to a sparse vector [4], [5]. Leveraging advances in signal processing, such as Compressing Sensing (CS) [6], allows to accelerate the recovery process by using less data. Moreover, theses methods build a more precise model of the backscattered signals. Still, a drawback of these methods is that a preprocessing step is needed to remove the front wall echoes [7], [8]. It assumes the subspaces of front wall and target backscatted signals to be non-overlapping, which may not always be the case. The wall removal preprocessing step then consists in projecting the received signal onto the orthogonal complement of the wall's response subspace, which may also cancel some target returns. Clutter from inside of the imaged scene is also not modelled which may impede detection in a natural setting (i.e. without absorbing materials). This issue is linked to the fact that the rank of the interference also requires to be estimated within the preprocessing step.

We consider a one-step method based on joint low-rank and sparse matrix recovery methods, introduced in the Robust PCA (RPCA) framework [9], [10]. It has been extended to include a dictionary for the sparse component in [11]. In our context, this allows a one-step recovery of target positions in the sparse component with the interferences captured by the low-rank component. This joint recovery approach for TWRI applications has been investigated in [12]–[14].

As suggested in [15], we start in the footsteps of RPCA 'with dictionary' (dRPCA) [11], where a linear operator is applied on the sparse component. Our model for this dictionary follows the one of [5]. Unfortunately, dRPCA is not able to recover the target positions in our simulations setting due to the highly structured sparse component. Then, to achieve the recovery of target positions, we propose a reformulation of dRPCA through a natural Kronecker product structured model which is solved with a corresponding modified ADMM algorithm [16].

In this paper, we add multipath considerations and reshape the data in its matrix form following the RPCA setting. As done in previous sparse recovery methods [17], we make use of a $\ell_{2,1}$ norm regularization to take multipath into account. In RPCA (without dictionary), this has been studied as 'outlier pursuit' [18] and shown to well recover the column support of the sparse component and the column space of the low-rank component. We also make use of CS to reduce data usage and speed up calculations, albeit naively. We validate and compare our model on simulations which confirmed that our proposed method correctly recovers target positions.

The paper is organized as follows: in Section II the signal model is introduced. Limitations of dRPCA are pointed out and a new method is proposed in Section III, leading to a modified RPCA problem. Finally, Section IV studies the performance of our new method in comparison with the

method of [5] which we denote SR-CS, as well as BP.

Let $\mathbf{A}$ be a complex-valued matrix with $(i,j)^{th}$ entry be denoted: $[\mathbf{A}]_{i,j} = a_{ij}$, i^{th} column be denoted $\mathbf{a}_i$ and i^{th} row be: $\mathbf{A}_{i,:}$. Further on, we denote by $\|\cdot\|_p$ the entrywise ℓ_p norm of a matrix. We denote the Frobenius norm as $\|\cdot\|_F$. The $\ell_{2,1}$-norm is $\|\mathbf{A}\|_{2,1} = \sum_i \left(\sum_j |a_{ij}|^2\right)^{1/2} = \sum_i \|\mathbf{A}_{i,:}\|_2$. Denote $\mathbf{A} \overset{\text{SVD}}{=} \mathbf{U}\mathbf{\Sigma}\mathbf{V}^H$ the SVD of $\mathbf{A}$. Then, the nuclear norm of $\mathbf{A}$ is $\|\mathbf{A}\|_* = \|\text{diag}\,(\mathbf{\Sigma})\|_1$ i.e. the sum of the singular values.

II. Through The Wall model

We consider a homogeneous wall of thickness d and dielectric constant ϵ located along the x-axis at a distance z_{off} to the SAR transceivers. Consider a N-element array with the n^{th} transceiver located at $\mathbf{x}_n = (x_n, -z_{off})$ sending a stepped-frequency signal of M equispaced frequencies over the band $[\omega_0; \omega_{M-1}]$, $\omega_m = \omega_0 + m\Delta\omega, \quad m = 0, 1, \ldots, M-1$ with $\Delta\omega$ the frequency step. The reflections from targets are measured only at the same transceiver position.

The received signal backscattered from targets and the front wall, at the n^{th} transceiver for the m^{th} frequency can be formulated as [5]:

$$\begin{aligned} y(m,n) &= \sigma_w \exp\left(-j\omega_m \tau_w\right) \\ &+ \sum_{i=0}^{R-1} \sum_{p=0}^{P-1} \sigma_p^{(i)} \exp(-j\omega_m \tau_{p,n}^{(i)}) \end{aligned} \tag{1}$$

where P is the number of point targets and R trajectories of multipath, σ_w is the complex-valued reflectivity of the wall and $\tau_w = \frac{2z_{off}}{c}$ is the round trip propagation delay from SAR transceiver to wall, with c the velocity of electromagnetic wave in the air medium. Moreover, $\sigma_p^{(i)}$ is a complex-valued attenuation coefficient which factors in the different losses for the i^{th} multipath to the p^{th} target: the wall refraction loss, path loss in air and wall, and target reflection loss. The two-way propagation delay from n^{th} transceiver to the p^{th} target along the i^{th} multipath is denoted $\tau_{p,n}^{(i)}$. The direct trajectory through the front wall can be computed by numerical methods [19], which allows to evaluate the associated wave propagation delay.

Assume the scene to be imaged is divided into a grid of dimension $N_x \times N_z$ in crossrange vs downrange. We now denote $\tau_{n_x n_z, n}^{(i)}$ the propagation delay to the $(n_x, n_z)^{th}$ pixel for the i^{th} multipath scheme and the n^{th} transceiver position. We can write the received signal through a dictionary $\mathbf{\Psi}$ which maps the whole scene. For the i^{th} multipath scheme and the n^{th} transceiver position, its m^{th} row is denoted:

$$[\mathbf{\Psi}_n^{(i)}]_m = [\exp\left(-j\omega_m \tau_{00,n}^{(i)}\right) \ldots \exp\left(-j\omega_m \tau_{(N_x N_z - 1),n}^{(i)}\right)] \tag{2}$$

This gives a vector form to the signal received at the n^{th} position:

$$\begin{aligned} \mathbf{y}_n &= \mathbf{l} + \underbrace{[\mathbf{\Psi}_n^{(0)} \mathbf{\Psi}_n^{(1)} \ldots \mathbf{\Psi}_n^{(R-1)}]}_{=\mathbf{\Psi}_n} \underbrace{\begin{bmatrix} \mathbf{r}^{(0)} \\ \mathbf{r}^{(1)} \\ \vdots \\ \mathbf{r}^{(R-1)} \end{bmatrix}}_{=\mathbf{r}} \\ \implies \mathbf{y}_n &= \mathbf{l} + \mathbf{\Psi}_n \mathbf{r} \end{aligned} \tag{3}$$

where $\mathbf{l} \in \mathbb{C}^M$ contains the returns of the front wall and $\mathbf{r}^{(i)} \in \mathbb{C}^{N_x N_z}$ is the scene vector associated to the i^{th} multipath propagation scheme: containing the backscattered signal amplitudes, it is non-zero only when a target is located at a given position in the grid. $\mathbf{\Psi}_n^{(i)} \in \mathbb{C}^{M \times N_x N_z}$ is the dictionary mapping from received signal to target positions, with propagation delay computed according to the i^{th} multipath scheme from the n^{th} transceiver position.

SR-CS requires that the front wall echoes have been filtered by some preprocessing. This is equivalent to considering that $\mathbf{l} = \mathbf{0}$. Thus, the problem is:

$$\begin{bmatrix} \mathbf{y}_0 \\ \mathbf{y}_1 \\ \vdots \\ \mathbf{y}_{N-1} \end{bmatrix} \overset{\text{def}}{=} \mathbf{y} = [\mathbf{\Psi}^{(0)} \mathbf{\Psi}^{(1)} \ldots \mathbf{\Psi}^{(R-1)}] \ \mathbf{r} \tag{4}$$

with the submatrices composing the dictionary constructed by considering one multipath at a time ($\mathbf{\Psi}^{(i)} = [\mathbf{\Psi}_0^{(i)T} \mathbf{\Psi}_1^{(i)T} \ldots \mathbf{\Psi}_{N-1}^{(i)T}]^T$ is the sub-dictionary associated to the i^{th} multipath). The recovery of $\mathbf{r}$ through this inversion problem, with a sparsity penalization, is a staple of sparse recovery/regression:

$$\min_{\mathbf{r}} \ \|\text{unvec}(\mathbf{r})\|_{2,1} \text{ s.t. } \mathbf{y} = [\mathbf{\Psi}^{(0)} \mathbf{\Psi}^{(1)} \ldots \mathbf{\Psi}^{(R-1)}] \ \mathbf{r} \tag{5}$$

with $\text{unvec}(\mathbf{r}) \overset{\text{def}}{=} [\mathbf{r}^{(0)} \mathbf{r}^{(1)} \ldots \mathbf{r}^{(R-1)}] \in \mathbb{C}^{N_x N_z \times R}$.

The $\ell_{2,1}$-norm penalty is used in order to promote block-sparsity across rows. Indeed, all scene vectors represent the same physical scene, although they include different propagation paths. Multipath ghosts appear as a response to one single target when multiple unstructured activations occur rather than a unique whole-row activation, i.e. factoring multipaths in $\mathbf{\Psi}$. Such structured penalty will thus favor factoring out these ghosts. An added compressive matrix, selecting random frequencies and transceiver positions, can be added for CS to be used.

To remove the front wall returns $\mathbf{l}$ and recover the target positions $\mathbf{r}$ in one-step, we do not consider a long vector concatenating all observations, but stack them in a matrix. We can concatenate the observations $\{\mathbf{y}_i\}_{i=0}^{N-1}$ in a matrix as:

$$\begin{aligned}\underbrace{[\mathbf{y}_0 \dots \mathbf{y}_{N-1}]}_{=\mathbf{Y}} &= \underbrace{[\mathbf{l} \dots \mathbf{l}]}_{=\mathbf{L}} + \\ &\underbrace{[\boldsymbol{\Psi}_0 \dots \boldsymbol{\Psi}_{N-1}]}_{=\boldsymbol{\Psi}} \underbrace{\begin{bmatrix} \mathbf{r} & \mathbf{0} & \dots & \mathbf{0} \\ \mathbf{0} & \ddots & \ddots & \vdots \\ \vdots & \ddots & \ddots & \mathbf{0} \\ \mathbf{0} & \dots & \mathbf{0} & \mathbf{r} \end{bmatrix}}_{=\mathbf{S}} \\ \implies \mathbf{Y} &= \mathbf{L} + \boldsymbol{\Psi}\mathbf{S} = \mathbf{L} + \boldsymbol{\Psi}\left(\mathbf{I}_N \otimes \mathbf{r}\right)\end{aligned} \tag{6}$$

where $\mathbf{Y} \in \mathbb{C}^{M \times N}$ is the data matrix, $\mathbf{L} \in \mathbb{C}^{M \times N}$ is a low-rank matrix of front wall returns, $\boldsymbol{\Psi} \in \mathbb{C}^{M \times N_x N_z RN}$ is a dictionary mapping to the target returns and $\mathbf{S} \in \mathbb{C}^{N_x N_z RN \times N}$ is the associated sparse matrix containing the scene vector.

The setting leads us to consider sparse and low-rank matrix decomposition methods.

III. Structured RPCA for TWRI

A. Problem formulation

From the model in the previous section, TWRI can be formulated as a low-rank plus (structured) sparse matrix recovery from noisy observations.

The decompositon of a matrix in low-rank and compressed sparse components is developed in [11], which we already referred to as dRPCA. It builds upon RPCA, whose original goal is to retrieve a low-dimensional subspace in which lie the data points, except for some outliers which are accounted for in a sparse matrix. It makes use of the ℓ_1 and nuclear norms which are known to be the convex envelopes of the ℓ_0 'norm' (the number of non-zeros entries) and rank of a (bounded) matrix [20]. It establishes recovery conditions of this convex relaxation, which can be solved through ADMM. The problem of dRPCA is:

$$\begin{aligned} \min_{\mathbf{L},\mathbf{S}} \quad & \|\mathbf{L}\|_* + \lambda \|\mathbf{S}\|_1 \\ \text{s.t.} \quad & \mathbf{Y} = \mathbf{L} + \boldsymbol{\Psi}\mathbf{S} \end{aligned} \tag{7}$$

which is shown to allow for the recovery of both components under some constraints.

In our application context, the matrix $\mathbf{S}$ is structured, which can be directly accounted for in the problem formulation. In fact, our experiments show that such reformulation is necessary because the composite block diagonal structure of $\mathbf{S}$ in (6) implies a strong sparsity pattern. Recovering this pattern from the unstructured formulation (7) causes convergence issues and leads to a failure of the target detection. From the model in (6), we therefore propose the following formulation:

$$\begin{aligned} \min_{\mathbf{L},\mathbf{r}} \quad & \|\mathbf{L}\|_* + \lambda \|\mathrm{unvec}(\mathbf{r})\|_{2,1} \\ \text{s.t.} \quad & \mathbf{Y} = \mathbf{L} + \boldsymbol{\Psi}\left(\mathbf{I}_N \otimes \mathbf{r}\right) \end{aligned} \tag{8}$$

In the following, we define $\mathbf{R} = \mathrm{unvec}(\mathbf{r})$ for ease of notation.

B. ADMM algorithm

We consider solving (8) through the Alternating Direction Method of Multipliers (ADMM) [16]. The augmented Lagrangian problem associated with (8) is:

$$\begin{aligned} l(\mathbf{L}, \mathbf{r}, \mathbf{U}) = & \|\mathbf{L}\|_* + \lambda \|\mathbf{R}\|_{2,1} \\ & + \langle \mathbf{U}, \mathbf{Y} - \mathbf{L} - \boldsymbol{\Psi}(\mathbf{I}_N \otimes \mathbf{r}) \rangle \\ & + \frac{\mu}{2} \|\mathbf{Y} - \mathbf{L} - \boldsymbol{\Psi}(\mathbf{I}_N \otimes \mathbf{r})\|_F^2 \end{aligned} \tag{9}$$

where $\mathbf{U}$ is the matrix of Lagrange multipliers associated with the constraint, λ is the sparsity regularization parameter and μ is the augmented Lagrangian penalty parameter. The following subsections will detail the update of each variables for minimizing $l(\mathbf{L}, \mathbf{r}, \mathbf{U})$.

1) Update $\mathbf{L}$*:* Assuming $\mathbf{r}$ and $\mathbf{U}$ fixed, the $\mathbf{L}$-minimisation step corresponds to the problem:

$$\begin{aligned} \min_{\mathbf{L}} \quad & \|\mathbf{L}\|_* + \langle \mathbf{U}, \mathbf{Y} - \mathbf{L} - \boldsymbol{\Psi}(\mathbf{I}_N \otimes \mathbf{r}) \rangle \\ & + \frac{\mu}{2} \|\mathbf{Y} - \mathbf{L} - \boldsymbol{\Psi}(\mathbf{I}_N \otimes \mathbf{r})\|_F^2 \end{aligned} \tag{10}$$

Its resolution is identical to the one of RPCA, which is obtained by the so-called singular value soft thresholding operator, the proximal [21] of the nuclear norm (with threshold λ), denoted D_λ. In fact, this is the ℓ_1-norm proximal (the so-called soft-thresholding operator S) applied on the singular values of a matrix. Recall $\mathbf{A} \overset{\text{SVD}}{=} \mathbf{U}\boldsymbol{\Sigma}\mathbf{V}^H$, so that: $D_\lambda(\mathbf{A}) = \mathbf{U} S_\lambda(\boldsymbol{\Sigma}) \mathbf{V}^H$, with the soft-thresholding operator, defined element-wise by: $[S_\lambda(\mathbf{A})]_{i,j} = \mathrm{sgn}(a_{ij}) \left(|a_{ij}| - \lambda\right)_+$ where $\mathrm{sgn}(a_{ij})$ is the (complex) sign function and $(x)_+ = \max(x, 0)$. The corresponding update for problem (10) is:

$$\mathbf{L}_{k+1} = D_{1/\mu}(\mathbf{Y} - \boldsymbol{\Psi}(\mathbf{I}_N \otimes \mathbf{r}_k) + \mu^{-1}\mathbf{U}_{k+1}). \tag{11}$$

2) Update $\mathbf{r}$*:* Assuming $\mathbf{L}$ and $\mathbf{U}$ fixed, the $\mathbf{r}$-minimisation step is formuated as:

$$\min_{\mathbf{r}} \quad \lambda \|\mathbf{R}\|_{2,1} + \mu \langle \boldsymbol{\Gamma}, \boldsymbol{\Psi}(\mathbf{I}_N \otimes \mathbf{r}) \rangle + \frac{\mu}{2} \|\boldsymbol{\Psi}(\mathbf{I}_N \otimes \mathbf{r})\|_F^2 \tag{12}$$

with $\boldsymbol{\Gamma} = \mathbf{L} - \mathbf{Y} - \mu^{-1}\mathbf{U}$. For the linear term, notice that:

$$\boldsymbol{\Psi}(\mathbf{I}_N \otimes \mathbf{r}) = \begin{bmatrix} (\boldsymbol{\Psi}_0)_{0,:}\mathbf{r} & \dots & (\boldsymbol{\Psi}_{N-1})_{0,:}\mathbf{r} \\ \vdots & \ddots & \vdots \\ (\boldsymbol{\Psi}_0)_{M-1,:}\mathbf{r} & \dots & (\boldsymbol{\Psi}_{N-1})_{M-1,:}\mathbf{r} \end{bmatrix} \tag{13}$$

with $\boldsymbol{\Psi}_{i,:} = [(\boldsymbol{\Psi}_0)_{i,:} (\boldsymbol{\Psi}_1)_{i,:} \dots (\boldsymbol{\Psi}_{N-1})_{i,:}]$. This leads to:

$$\begin{aligned} \langle \boldsymbol{\Gamma}, \boldsymbol{\Psi}(\mathbf{I}_N \otimes \mathbf{r}) \rangle &= \mathrm{Tr}\left(\boldsymbol{\Gamma}^H \boldsymbol{\Psi}(\mathbf{I}_N \otimes \mathbf{r})\right) \\ &= \mathrm{vec}\left(\boldsymbol{\Gamma}\right)^H \mathrm{vec}\left(\boldsymbol{\Psi}(\mathbf{I}_N \otimes \mathbf{r})\right) \\ &= \underbrace{\sum_{i=0}^{M-1} \sum_{j=0}^{N-1} (\overline{\gamma_{ij}} (\boldsymbol{\Psi}_j)_{i,:})}_{=\mathbf{n}^H} \mathbf{r} = \langle \mathbf{n}, \mathbf{r} \rangle \end{aligned} \tag{14}$$

Algorithm 1 ADMM for RPCA with a sparse vector and Kronecker structure $(\lambda, \mu, \mathbf{Y}, \mathbf{\Psi})$

$\mathbf{L}_0, \mathbf{U}_0 \leftarrow \mathbf{0}_{M\times N}$
$\mathbf{r}_0 \leftarrow \mathbf{0}_{N_x N_z \times 1}$
$\mathbf{P} = \sum_{i=0}^{N-1} \mathbf{\Psi}_i^H \mathbf{\Psi}_i$
$t = 1/\lambda_{\max}(\mu\mathbf{P})$
repeat (for $k = 0, 1, \ldots$):
  $\mathbf{U}_{k+1} = \mathbf{U}_k + \mu(\mathbf{Y} - \mathbf{L}_k - \mathbf{\Psi}(\mathbf{I}_N \otimes \mathbf{r}_k))$
  $\mathbf{L}_{k+1} = D_{1/\mu}(\mathbf{Y} - \mathbf{\Psi}(\mathbf{I}_N \otimes \mathbf{r}_k) + \mu^{-1}\mathbf{U}_{k+1})$
  $\mathbf{\Gamma} = \mathbf{L}_{k+1} - \mathbf{Y} - \mu^{-1}\mathbf{U}_{k+1}$
  $\mathbf{n} = \sum_{i=0}^{M-1}\sum_{j=0}^{N-1} (\mathbf{\Gamma})_{i,j}[(\mathbf{\Psi}_j)_{i:}]^H$
  repeat (for $q = 0, 1, \ldots$):
    $\mathbf{R}_{q+1} = T_{\lambda t}(\text{unvec}(\mathbf{r}_q - t\mu(\mathbf{n} + \mathbf{P}\mathbf{r}_q)))$
    $\mathbf{r}_{q+1} = \text{vec}\,(\mathbf{R}_{q+1})$
  until stopping criterion is met
  $\mathbf{r}_{k+1} \leftarrow \mathbf{r}_{q+1}$
until stopping criterion is met
$\mathbf{L} \leftarrow \mathbf{L}_{k+1}$
$\mathbf{r} \leftarrow \mathbf{r}_{k+1}$

where $\gamma_{ij} = [\mathbf{\Gamma}]_{i,j}$. Concerning the quadratic term, we have:

$$\begin{aligned}\|\mathbf{\Psi}(\mathbf{I}_N \otimes \mathbf{r})\|_F^2 &= \text{Tr}\,(\mathbf{\Psi}^H\mathbf{\Psi}(\mathbf{I}_N \otimes \mathbf{r})(\mathbf{I}_N \otimes \mathbf{r}^H)) \\ &= \text{Tr}\,(\mathbf{\Psi}^H\mathbf{\Psi}(\mathbf{I}_N \otimes \mathbf{r}\mathbf{r}^H)) \\ &= \sum_{i=0}^{N-1} \text{Tr}\,(\mathbf{\Psi}_i^H\mathbf{\Psi}_i\mathbf{r}\mathbf{r}^H) = \mathbf{r}^H\mathbf{P}\mathbf{r}\end{aligned} \tag{15}$$

where $\mathbf{P} = \sum_{i=0}^{N-1} \mathbf{\Psi}_i^H\mathbf{\Psi}_i$ is positive-semidefinite matrix. We get that the $\mathbf{r}$-minimization step (12) can be written as:

$$\min_{\mathbf{r}} \quad l(\mathbf{L}, \mathbf{r}, \mathbf{U}) = \lambda\|\mathbf{R}\|_{2,1} + \mu\langle\mathbf{n}, \mathbf{r}\rangle + \frac{\mu}{2}\mathbf{r}^H\mathbf{P}\mathbf{r} \tag{16}$$

Thus, the $\mathbf{r}$-minimization step is a sum of convex functions with known gradients. This $\mathbf{r}$-minimization step can be achieved through (possibly accelerated) proximal gradient descent [21, Section 4.2]. At iteration q:

$$\mathbf{R}_{q+1} = T_{\lambda t}(\text{unvec}(\mathbf{r}_q - t\mu(\mathbf{n} + \mathbf{P}\mathbf{r}_q))) \tag{17}$$

where $T_\lambda(\cdot)$ denotes the proximal operator of the $\ell_{2,1}$ norm, defined row by row, by: $[T_\lambda(\mathbf{A})]_{i,:} = \left(1 - \frac{\lambda}{\|\mathbf{A}_{i,:}\|_2}\right)_+ \mathbf{A}_{i,:}$.

3) Update $\mathbf{U}$*:* This is a standard ADMM step of dual ascent: $\mathbf{U}_{k+1} = \mathbf{U}_k + \mu(\mathbf{Y} - \mathbf{L}_k - \mathbf{\Psi}(\mathbf{I}_N \otimes \mathbf{r}_k))$

The whole method is summarized in Algorithm 1.

IV. Simulations

We test our method on simulated data. The scene is 4.9×5.4 m in crossrange (x-axis) vs downrange (z-axis). The stepped-frequency signal is composed of 728 frequencies from 1 GHz to 3 GHz. The SAR moves along the x-axis between each acquisition with 67 different positions overall. Its track is centered over the x-axis, thus it starts around $x = 1.82$ and ends at $x = 3.05$. The front wall (which is parallel to the SAR displacement axis) is at a standoff distance to the SAR of 1.2 m, of thickness 0.5 m, of relative permittivity $\epsilon = 4.5$. The front wall returns have around 40 dB overall attenuation. Two targets are situated at (x, z) coordinates $(2, 2)$ and $(2.5, 4)$ with overall attenuation around 70 dB for the direct path (this loss includes free space path loss, losses through the front wall as well as losses due to the target) based on [1, Section 2.2]. For every other multipath, we add an extra attenuation coefficient. The Signal to Noise Ratio (SNR) is set to 20 dB with noise modelled by a complex Gaussian white noise.

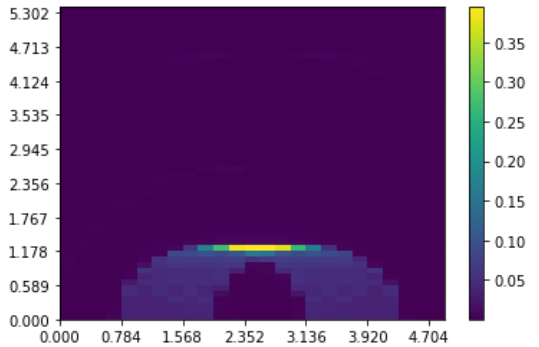

Fig. 1: Result of BP

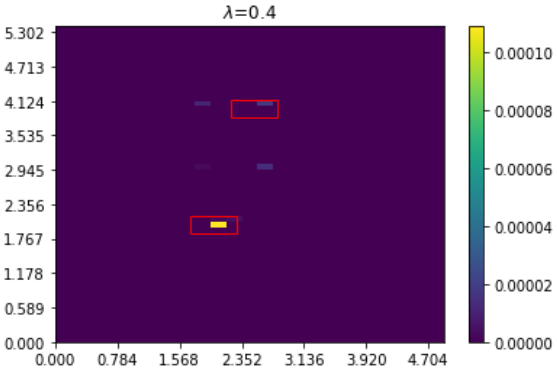

Fig. 2: Result of SR-CS ($\lambda = 0.4$)

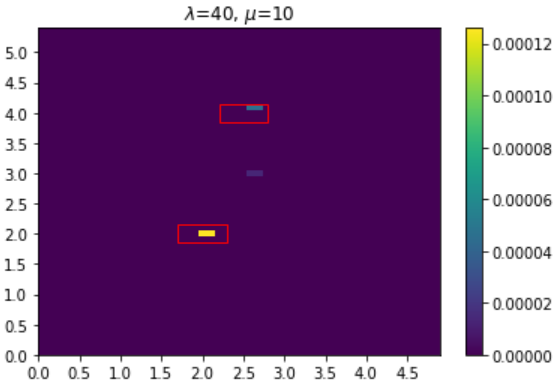

Fig. 3: Result of kRPCA ($\lambda = 40, \mu = 10$)

With some multipath (wall ringing), a standard SAR method such as BP achieves a result as seen on Figure 1. The wall returns are overwhelming.

The method of SR-CS achieves the result seen on Figure 2. The wall returns have been mitigated by the subspace projection method of [7], although without noise suppression nor mean signal removal as it degraded performance. A compressive matrix is used to select 25% of frequencies. The true target positions are indicated by the red rectangular boxes. The results of our method, which we denote kRPCA, is shown on on Figure 3 with a compressive matrix used to select frequencies, with 25% being kept.

For more reprensative results, we run a Monte-Carlo simulation over a range of SNR. We use 100 draws at each SNR, and stop each method at iterate k when two iterates are close by: $\left\|\mathbf{r}^k - \mathbf{r}^{k-1}\right\|_F \leq 1\mathrm{e}^{-6}$. This generally amounts to around 20 iterations for both algorithms. The error evaluated is defined as the count of false alarms plus non-detections. To this end, we consider blocks of 2 by 2 pixels to allow for small clusters of pixels and set a detection threshold to 10 % the highest pixel intensity. The hyperparameters are set to a value manually found to be optimal and remain constant over all draws. We observe in Figure 4 that our method performs better than SR-CS, as our error tends to zero while SR-CS stays around one. The likely reason is that the ghost target (visible on the previous images) is difficult to erase for SR-CS.

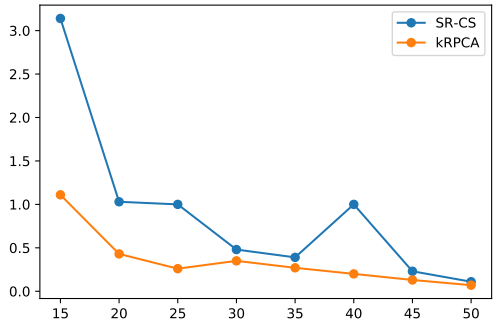

Fig. 4: Estimated error as a function of SNR (dB)

Also note that in order to keep a readable scale, we do not show smaller SNR values as the error of SR-CS goes in the hundreds whereas kRPCA remains below ten.

V. Conclusions

In this work, we proposed a novel one-step method for Through-the-Wall Radar Imaging. Formulated as a structured recovery problem in the form of a sparse plus low-rank decomposition, it is solved through a modification of the so-called Robust PCA 'with dictionary' (dRPCA). In this tailored adaptation, we make use of the Kronecker product structure of the sparse component, as well as its row-wise sparsity, to achieve its recovery. Simulations showed that our proposed method is able to achieve recovery of target positions with lower SNR than SR-CS [5]. Further performance evaluation of our method will be investigated on a real dataset with possibly unmitigated clutter.

References

[1] M. Amin, *Through-the-Wall Radar Imaging*. CRC Press, 2017. [Online]. Available: https://books.google.fr/books?id=JkzRBQAAQBAJ

[2] S. Kraut, L. L. Scharf, and L. T. McWhorter, "Adaptive subspace detectors," *IEEE Trans. Signal Process.*, vol. 49, pp. 1–16, 2001.

[3] M. Soumekh, "Synthetic aperture radar signal processing with matlab algorithms," 1999.

[4] Q. Huang, L. Qu, B. Wu, and G. Fang, "Uwb through-wall imaging based on compressive sensing," *IEEE Transactions on Geoscience and Remote Sensing*, vol. 48, no. 3, pp. 1408–1415, 2010.

[5] M. G. Amin and F. Ahmad, "Compressive sensing for through-the-wall radar imaging," *Journal of Electronic Imaging*, vol. 22, no. 3, pp. 1 – 22, 2013. [Online]. Available: https://doi.org/10.1117/1.JEI.22.3.030901

[6] S. Foucart and H. Rauhut, "An invitation to compressive sensing," in *A mathematical introduction to compressive sensing*. Springer, 2013, pp. 1–39.

[7] F. H. C. Tivive, A. Bouzerdoum, and M. G. Amin, "A subspace projection approach for wall clutter mitigation in through-the-wall radar imaging," *IEEE Transactions on Geoscience and Remote Sensing*, vol. 53, no. 4, pp. 2108–2122, 2015.

[8] P. K. Verma, A. N. Gaikwad, D. Singh, and M. Nigam, "Analysis of clutter reduction techniques for through wall imaging in uwb range," *Progress In Electromagnetics Research B*, vol. 17, pp. 29–48, 2009.

[9] E. J. Candès, X. Li, Y. Ma, and J. Wright, "Robust principal component analysis?" *Journal of the ACM (JACM)*, vol. 58, no. 3, pp. 1–37, 2011.

[10] V. Chandrasekaran, S. Sanghavi, P. A. Parrilo, and A. S. Willsky, "Rank-sparsity incoherence for matrix decomposition," *SIAM Journal on Optimization*, vol. 21, no. 2, p. 572–596, Apr 2011. [Online]. Available: http://dx.doi.org/10.1137/090761793

[11] M. Mardani, G. Mateos, and G. B. Giannakis, "Recovery of low-rank plus compressed sparse matrices with application to unveiling traffic anomalies," *IEEE Transactions on Information Theory*, vol. 59, no. 8, p. 5186–5205, Aug 2013. [Online]. Available: http://dx.doi.org/10.1109/TIT.2013.2257913

[12] Y. Zhang and T. Xia, "In-wall clutter suppression based on low-rank and sparse representation for through-the-wall radar," *IEEE Geoscience and Remote Sensing Letters*, vol. 13, no. 5, pp. 671–675, 2016.

[13] V. H. Tang, A. Bouzerdoum, S. L. Phung, and F. H. C. Tivive, "Radar imaging of stationary indoor targets using joint low-rank and sparsity constraints," in *2016 IEEE International Conference on Acoustics, Speech and Signal Processing (ICASSP)*, 2016, pp. 1412–1416.

[14] V. H. Tang, A. Bouzerdoum, and S. L. Phung, "Compressive radar imaging of stationary indoor targets with low-rank plus jointly sparse and total variation regularizations," *IEEE Transactions on Image Processing*, vol. 29, pp. 4598–4613, 2020.

[15] B. Mériaux, A. Breloy, C. Ren, M. N. El Korso, and P. Forster, "Modified sparse subspace clustering for radar detection in non-stationary clutter," in *2019 IEEE 8th International Workshop on Computational Advances in Multi-Sensor Adaptive Processing (CAMSAP)*, 2019, pp. 669–673.

[16] S. Boyd, N. Parikh, E. Chu, B. Peleato, and J. Eckstein, "Distributed optimization and statistical learning via the alternating direction method of multipliers," *Found. Trends Mach. Learn.*, vol. 3, no. 1, p. 1–122, Jan. 2011. [Online]. Available: https://doi.org/10.1561/2200000016

[17] M. Leigsnering, F. Ahmad, M. Amin, and A. Zoubir, "Multipath exploitation in through-the-wall radar imaging using sparse reconstruction," *IEEE Transactions on Aerospace and Electronic Systems*, vol. 50, no. 2, pp. 920–939, 2014.

[18] H. Xu, C. Caramanis, and S. Sanghavi, "Robust pca via outlier pursuit," ser. NIPS'10. Red Hook, NY, USA: Curran Associates Inc., 2010, p. 2496–2504.

[19] F. Ahmad and M. G. Amin, "Noncoherent approach to through-the-wall radar localization," *IEEE Transactions on Aerospace and Electronic Systems*, vol. 42, no. 4, pp. 1405–1419, 2006.

[20] M. Fazel, "Matrix rank minimization with applications," Ph.D. dissertation, PhD thesis, Stanford University, 2002.

[21] N. Parikh and S. Boyd, "Proximal algorithms," *Found. Trends Optim.*, vol. 1, no. 3, p. 127–239, Jan. 2014. [Online]. Available: https://doi.org/10.1561/2400000003